Journal of Chromatography, 260 (1983) 391–409
Elsevier Science Publishers B.V., Amsterdam — Printed in The Netherlands

CHROM. 15,650

CHARACTERIZATION OF HYDROCARBON WAXES BY GAS–LIQUID CHROMATOGRAPHY WITH A HIGH-RESOLUTION GLASS CAPILLARY COLUMN

HIROSHI NAKAGAWA and SHIN TSUGE*
Department of Synthetic Chemistry, Faculty of Engineering, Nagoya University, Nagoya 464 (Japan)
and
TOMOMITSU ITHO and MITSUO KIMOTO
Chukyo Fat and Oil Company, Tomikawa-cho 2-1, Nakagawa-ku, Nagoya 454 (Japan)
(Received December 27th, 1982)

SUMMARY

Sixteen hydrocarbon waxes of four different types were characterized by high-resolution glass capillary gas chromatography (GC) coupled with a direct vaporizer for solid samples. A furnace-type pyrolyser is used as the vaporizer. Components having very similar structures, such as branched-chain alkanes and the corresponding *n*-alkanes, were clearly separated using a high-resolution glass capillary column. The resulting GC data were correlated with various physical properties of the waxes, such as melting point, refractive index, degree of needle penetration and specific gravity. Thermogravimetric analysis and other thermal methods were also used to determine the molecular weight distributions and average molecular weights of the waxes.

INTRODUCTION

Waxes have been used extensively in making candles and they are widely used in industry in adhesives, electrical insulations, coatings, lubricants, etc. Waxes can be classified into four groups: (1) animal and vegetable waxes; (2) petroleum waxes; (3) mineral waxes; and (4) synthetic waxes. The petroleum waxes, which are mainly used in industry, are further classified into paraffin waxes and microcrystalline waxes. The paraffin waxes fractionated from crude petroleum are mixtures of mainly *n*-alkanes with minor amounts of branched-chain alkanes and cycloalkanes. Their average molecular weights mostly range from about 350 to 450. Microcrystalline waxes are prepared from the reduced pressure distillation residues of crude petroleum and their chemical components are said to be mainly branched-chain alkanes. The average molecular weights of microcrystalline waxes range from about 550 to 700. Synthetic waxes, including low-molecular-weight polyethylenes, generally have higher average molecular weights than the petroleum waxes, ranging from about 500 to 10,000[1].

Various analytical methods, such as gel permeation chromatography, differential scanning calorimetry (DSC), infrared (IR) spectroscopy, mass spectrometry (MS)

0021-9673/83/$03.00 © 1983 Elsevier Science Publishers B.V.

and gas chromatography (GC) have been employed in the characterization of waxes. GPC[2] has been used for molecular weight distribution measurements of waxes. IR spectroscopy[3] gives useful information on the differences between paraffin waxes and microcrystalline waxes. DSC[4] offers a means of classifying different types of waxes. Although these methods are applicable to high-boiling-point waxes, they are not so effective in elucidating the microstructures. MS[5] gives information on two important features of waxes, *viz.*, the molecular weight distributions and the molecular types present, although the resulting mass spectra do not always correspond directly to the distributions of the components because of the associated fragmentation.

GC, on the other hand, is a highly effective characterization technique with simple equipment, particularly when applied to relatively low-boiling waxes. Early GC work by Ludwig[6] was carried out with a conventional packed column, with which the chromatograms of the urea-adductable fraction of microcrystalline waxes were obtained. Recent GC work by Lawrence *et al.*[7] refers to the characterization of vegetable and animal waxes using stepwise pre-treatments such as esterification and acetylation. However, components having similar structures could not be separated satisfactorily using a packed column. On the other hand, in order to utilize a high-resolution capillary column, special care has to be taken to achieve quantitative sample introduction for high-boiling components such as waxes. Additionally in this instance, the stationary phase is expected to have as high a thermal stability as possible to cover even the higher boiling components in the waxes.

In this work, in order to overcome these problems sample introduction into a gas chromatograph was carried out by use of a furnace-type pyrolyser as a vaporizing device and GC separation was performed using a glass capillary column coated with Dexile 300-GC. By this method, *n*-alkanes with over 50 carbon atoms could be almost completely separated from the corresponding branched-chain alkanes and errors encountered with syringe injection of the sample solution on to the capillary column could be avoided as solid wax is vaporized directly in the vaporizing device under a flow of inert carrier gas (nitrogen) at high temperatures with mininmal thermal degradation. The physical properties of the waxes, such as melting point, refractive index, penetration and specific gravity are discussed in connection with the GC data. Thermogravimetric analysis (TGA) and other thermal methods were also employed to measure the thermal behaviour of the waxes.

EXPERIMENTAL

Samples

The waxes used are listed in Table I together with their physical properties.

GC conditions

A schematic diagram of the GC system is shown in Fig. 1. The vaporizer (Yanagimoto GP-1018 pyrolyser) directly attached to a gas chromatograph (Yanagimoto G-3800) is used in the same way as in the pyrolysis GC of polymer samples. Details of the vaporizer are shown in Fig. 2. A small amount of a solid sample is mounted in the platinum sample holder (Fig. 2D), which is fitted in the chuck (Fig. 2B). By pushing the button (Fig. 2A), the sample holder is dropped to the centre of the furnace, which is maintained at a fixed vaporizing temperature between 400 and

TABLE I

WAXES AND THEIR PHYSICAL CONSTANTS

Wax sample	*Melting point (°C)*	*Refractive index*	*Penetration (× 0.1 mm)*	*Specific gravity*
Paraffin waxes:				
(A) NS-155°F*	69	1.432	24	0.917
(B) NS-140°F	61	1.425	19	0.909
(C) NS-130°F	56	1.424	29	0.908
(D) NR-155°F**	69	1.432	20	0.919
(E) NR-150 F	66	1.430	19	0.913
(F) NR-140°F	60	1.427	20	0.910
(G) NR-130°F	55	1.424	23	0.907
(H) NR-120°F	48	1.422	27	0.905
*Synthetic waxes****:*				
(I) Bareco Polywax 500	86	1.431	9	0.932
(J) Bareco Polywax 655	102	1.432	4	0.945
(K) Bareco Polywax 1000	113	1.432	4	0.952
Low-molecular-weight polyethylenes:				
(L) AC-PE 6§ (average molecular weight = 2000)	100	1.463	8	0.916
(M) AC-PE 615 (average molecular weight = 5000)	–	–	–	–
Microcrystalline waxes:				
(N) Multiwax X-145	60	1.445	65	0.910
(O) Multiwax 200M	93	1.445	10	0.930
(P) Mobile micro 190Y	–	–	–	–

* NS: Nihon Sekiyu.
** NR: Nihon Seiro.
*** Numbers represent the number-average molecular weights.
§ AC: Allied Chemical.

650°C. The vaporized sample components are transferred into a capillary column (30 m × 0.2 mm I.D. SCOT column, Dexile 300-GC) through a splitter by the flow of carrier gas. The resulting chromatogram is recorded, together with the corresponding peak area. The connection part between the vaporizer and the injection port has to be heated to prevent condensation of the high-boiling point components. Further, the splitter is also maintained at the final column temperature during the sample injection so as to split the whole range of the components quantitatively. To examine the quantitative and reproducible splitting, the data for polystyrene pyrolysates were used[7]. In order to protect the capillary column from high-boiling tarry components, the glass insert (Fig. 1L) was packed with support material coated with Dexile 300-GC and held at the final column temperature.[8]

The operating conditions for paraffin waxes and polyethylenes were as follows: temperature between vaporizer and injection port, 260°C; injector and splitter tem-

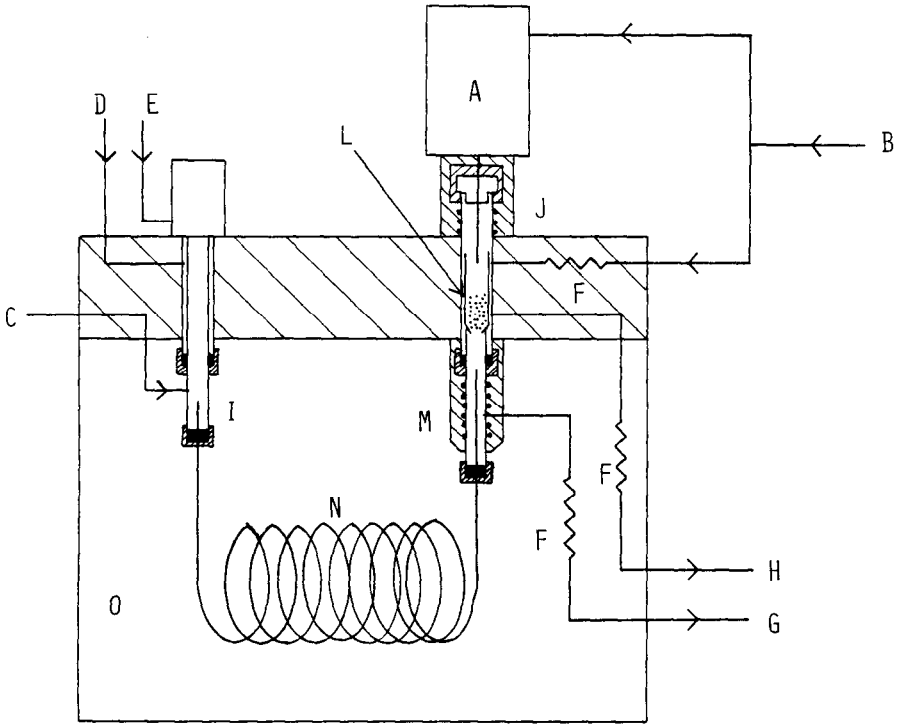

Fig. 1. Schematic diagram of GC system with a solid sample vaporizer. A = Vaporizer; B = carrier gas inlet; C = scavenger gas inlet; D = hydrogen inlet; E = air inlet; F = resistance tube; G = vent; H = ghost cut gas outlet; I = outlet tube; J = heat insulation; K = FID; L = glass insert with packing; M = splitter; N = glass capillary column; O = column oven.

perature, 300°C; column temperature, 50–300°C, programmed at 3°C/min; and scavenger gas flow-rate, 40 ml/min. About 100 μg of the paraffin wax or 300 μg of the polyethylene wax, weighed in the platinum sample holder, was vaporized under a flow of carrier gas (65 ml/min, splitting ratio 1:150) at the vaporizing temperature.

The operating conditions for microcrystalline waxes and synthetic waxes were as follows: temperature between vaporizer and injection port, 300°C; injector and splitter temperature, 350°C; column temperature, 50–350°C, programmed at 3°C/min; other conditions as for paraffin waxes.

TGA conditions

TGA was carried out using a Rigaku Denki thermobalance. About 9 mg of a sample weighed in a platinum sample holder was measured from room temperature to about 500°C at a rate of 10°C/min under a gentle flow of nitrogen.

Measurement of thermal vaporization curves with an FID

A schematic diagram for this method is shown in Fig. 3. Basically the same device as used in GC was used here, except for the separation column. In this instance, an empty copper tube (60 cm × 1.5 mm I.D.) was used instead of the capillary

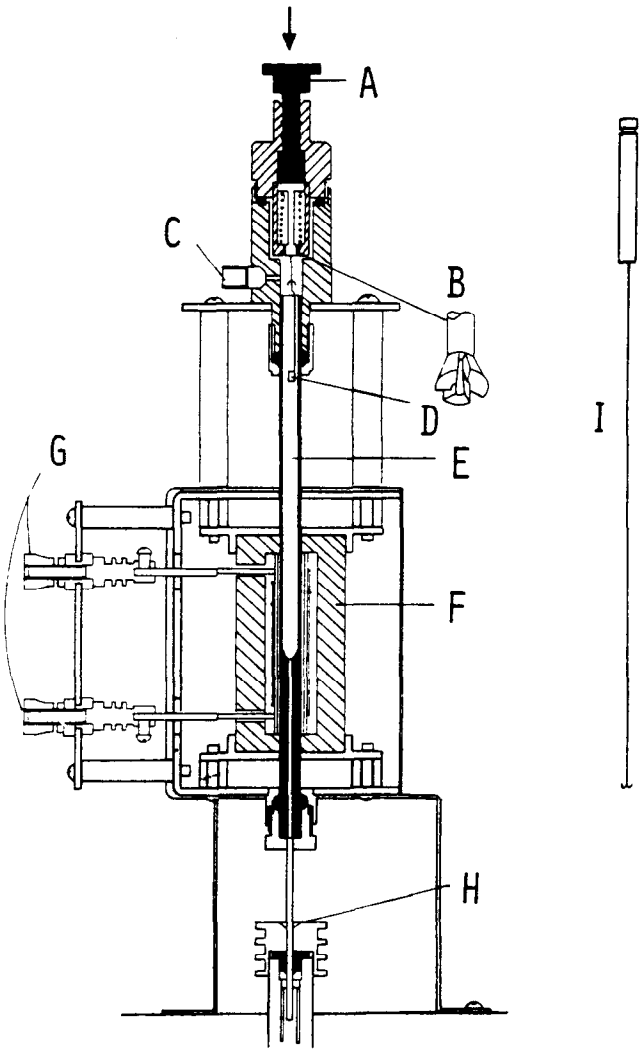

Fig. 2. Vertical microfurnace-type pyrolyser (vaporizer). A = Push-button; B = sample holder chuck; C = carrier gas inlet; D = sample holder; E = quartz tube; F = heat insulation; G = power supply; H = GC injection port; I = sample holder hook.

column. The vaporizer was maintained at a constant temperature of 400°C and the column oven and the injection port were maintained at 270°C and 300°C, respectively. A sample of about 100 μg was vaporized under a flow of nitrogen carrier gas at 65 ml/min.

Measurement of physical properties of the waxes

Refractive index measurements were made using an Atago 302 Abbé refractometer at 80°C. Penetration tests were carried out at 25°C by measuring the penetra-

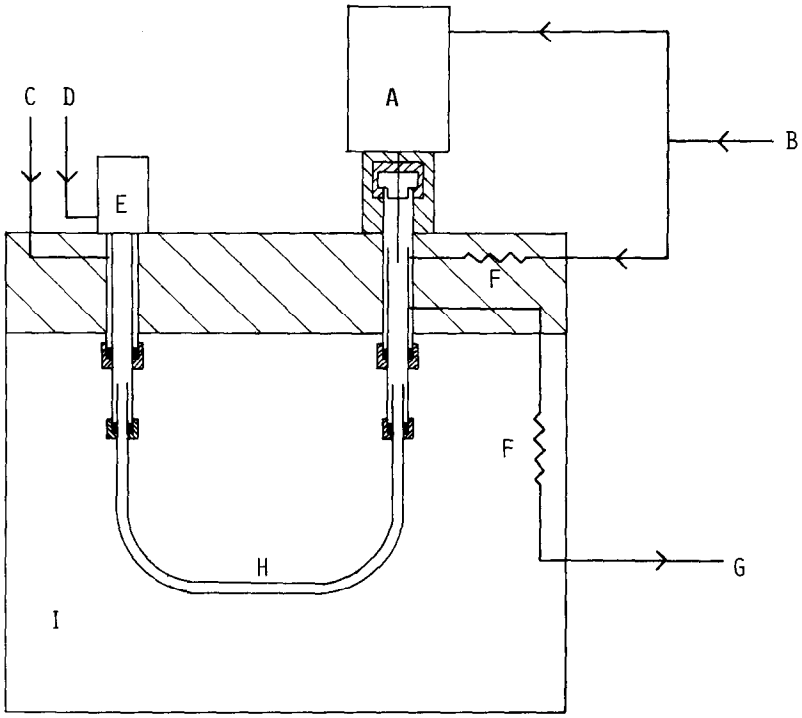

Fig. 3. Schematic diagram for measurement of thermal vaporization curves using FID. A = Vaporizer; B = carrier gas inlet; C = hydrogen inlet; D = air inlet; E = FID; F = resistance tube; G = ghost cut gas outlet; H = copper tube; I = column oven.

tion depth of a needle with a fixed top load (150 g) into the wax sample specified by Japan Industrial Standard (JIS) K3520.

Specific gravities of the solid waxes were measured according to the following method. The weight of a wax sample plus a weight was measured both in air and in a 0.5 % aqueous solution of 10 mol of ethylene oxide adduct with nonylphenol (NP-10 solution). The specific gravity of the wax is calculated using the equation

$$d = \frac{W_{a1} - W_{a2}}{[(W_{a1} - W_{a2}) - (W_{w1} - W_{w2})]/d_w} \quad (1)$$

where d is the specific gravity of the solid wax, W_{a1} and W_{a2} are the weights of the wax plus the weight and the weight alone measured in air, respectively, W_{w1} and W_{w2} are the weights of the wax plus the weight and the weight alone measured in the NP-10 solution, respectively, and d_w is the specific gravity of the solution.

The physical properties listed in Table I are mean values obtained by five replicate measurements. The wax samples for the penetration and the specific gravity measurements were prepared by moulding the melted waxes at 20°C above their melting points into an iron vessel (30 mm high × 31 mm I.D.).

RESULTS AND DISCUSSION

Study of fundamental GC conditions

The thermal vaporization of waxes is affected by various factors, such as vaporization temperature, flow-rate and pressure of the carrier gas. In order to achieve instantaneous vaporization of a wax sample with a wide volatility range, a relatively high temperature is usually applied. However, at elevated temperatures, undesirable thermal decomposition is accompanied by thermal vaporization. Therefore, a compromise vaporization temperature under given experimental GC conditions was first empirically determined by using NS-155°F as a test sample.

Fig. 4 shows relationships between the vaporizer temperature and the relative peak areas of C_1–C_5 components and the *n*-alkane peaks from C_{37} to C_{41} at a fixed flow-rate of the carrier gas (65 ml/min, splitting ratio 1:150). Of these, the C_1–C_5 components are a good measure of the contribution of thermal decomposition. The relative peak area of C_1–C_5 components increases gradually with increasing the vaporizer temperature, although it is below 1% when the vaporizer temperature is below 550°C. On the other hand, the relative peak areas of the C_{37}–C_{41} components show maxima when the vaporizer temperature is 550°C. These data suggest that the contribution of thermal decomposition becomes significant above 550°C, and that at lower temperatures the sample introduction is incomplete for the high-boiling components. The compromise vaporization temperature was therefore fixed at 550°C.

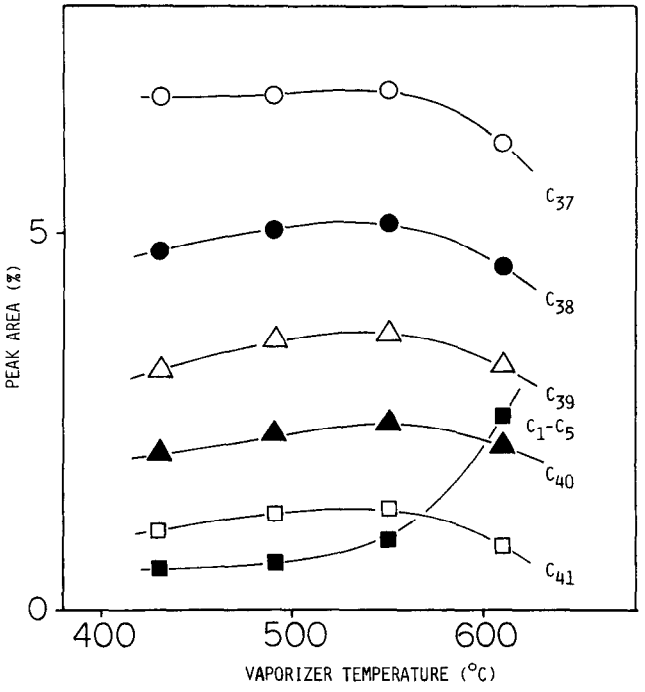

Fig. 4. Relationship between peak area and vaporizer temperature. Sample, paraffin wax NS-155°F; flow-rate of carrier gas, 65 ml/min.

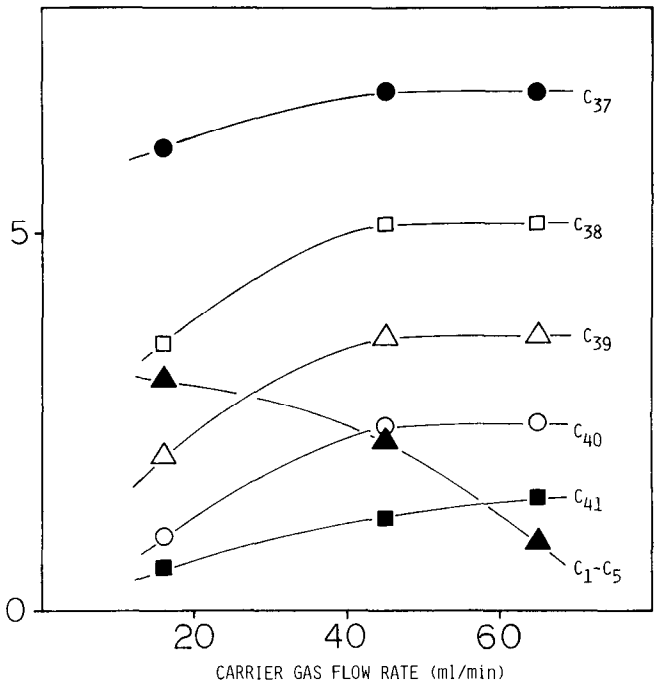

Fig. 5. Relationship between peak area and carrier gas flow-rate. Sample, as in Fig. 4; vaporization temperature, 550°C.

Fig. 5 shows relationships between the carrier gas flow-rate and the relative peak areas of C_1–C_5 and C_{37}–C_{41} components at a vaporization temperature of 550°C. The pressure of the carrier gas at the vaporizer was maintained at a relatively low value of 1.2 kg/cm^2 by changing the splitting ratio, as it was found that higher pressures resulted in an increase in thermal decomposition. The peak areas of the C_1–C_5 components decrease with increasing carrier gas flow-rate, whereas those of the C_{37}–C_{41} components show the opposite tendency. These data suggest that higher flow-rates of carrier gas are effective both in suppressing the thermal decomposition of the sample and in promoting the quantitative transfer of the vaporized wax components from the vaporizer to the separation column. Therefore, in subsequent work, a relatively high splitting ratio of 1:150 was employed to achieve the low pressure (1.2 kg/cm^2) and a high carrier gas flow-rate (65 ml/min) at the same time.

Finally, the quantitative detection of the sample components over a wide range of boiling points was examined using a Seeger and Gritter plot for polyethylene pyrolysates[9]. There must be a linear relationship between the logarithm of the molar peak intensities (*i.e.*, peak area/carbon number) and the carbon number of the peaks on the pyrogram of polyethylene. This linear relationship does not hold when high-boiling-point components are condensed in the GC system. The Seeger and Gritter plot of polyethylene obtained with the system used in this work is shown in Fig. 6. This plot suggests that the high-boiling components with over 40 carbon atoms are quantitatively introduced without any serious condensation or loss.

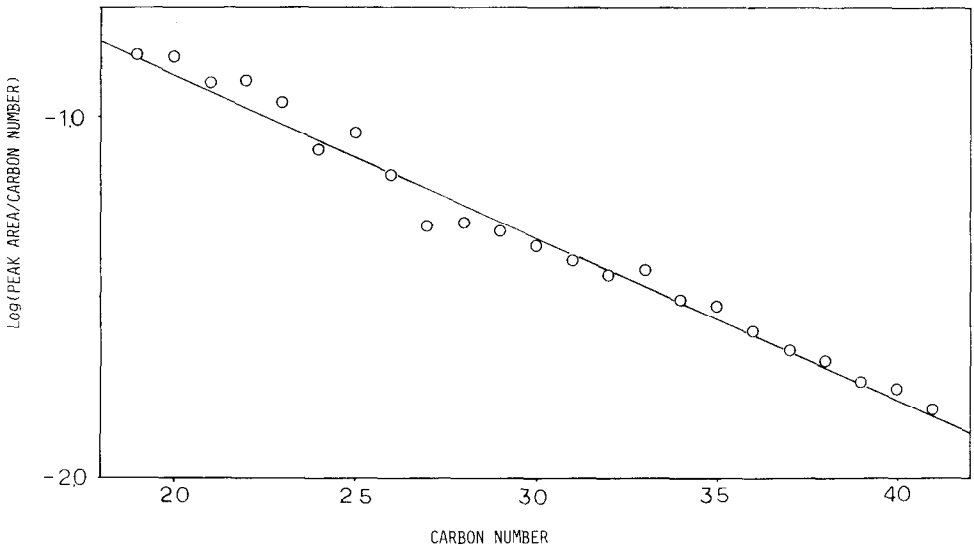

Fig. 6. Seeger and Gritter plot for polyethylene. Sample, high-density polyethylene; pyrolysis temperature, 550°C; flow-rate of carrier gas, 65 ml/min.

GC analysis of the waxes

Typical chromatograms of the paraffin waxes are shown in Fig. 7. The major peaks are *n*-alkanes and the small peaks between them are mostly isoalkanes. As the response of a flame-ionization detector (FID) for hydrocarbons is proportional to their carbon number, the observed relative peak intensities correspond directly to the original distributions of the constituents. Thus observed distributions of *n*-alkanes and isoalkanes are shown in Fig. 8. The total curves (solid lines) correspond to the molecular weight distribution of the waxes. In every instance the distribution of isoalkanes has a higher maximum than that of *n*-alkanes.

The number-average molecular weights ($\bar{M}_n$) of the waxes were calculated by the following equation and are summarized in Table II:

$$\bar{M}_n = \Sigma W_i / \Sigma (W_i / M_i) \tag{2}$$

where M_i is the molecular weight of the component i and W_i is the amount of the component. Here, the relative peak area of the corresponding peaks on the chromatograms was used instead of W_i. The isoalkane contents [C_{iso} (%)] of the waxes shown in Table II were calculated as follows:

$$C_{iso}\,(\%) = \Sigma W_i\,(\text{iso}) / \Sigma W_i \tag{3}$$

where ΣW_i (iso) corresponds to the total area of isoalkane peaks and ΣW_i to the total area of isoalkanes and *n*-alkanes. The isoalkane contents generally tend to increase with increasing $\bar{M}_n$, except for NR-120°F.

Chromatograms of synthetic waxes (Polywaxes) are shown in Fig. 9. The major components of Polywax 500 are even carbon number (even-C) *n*-alkanes, in-

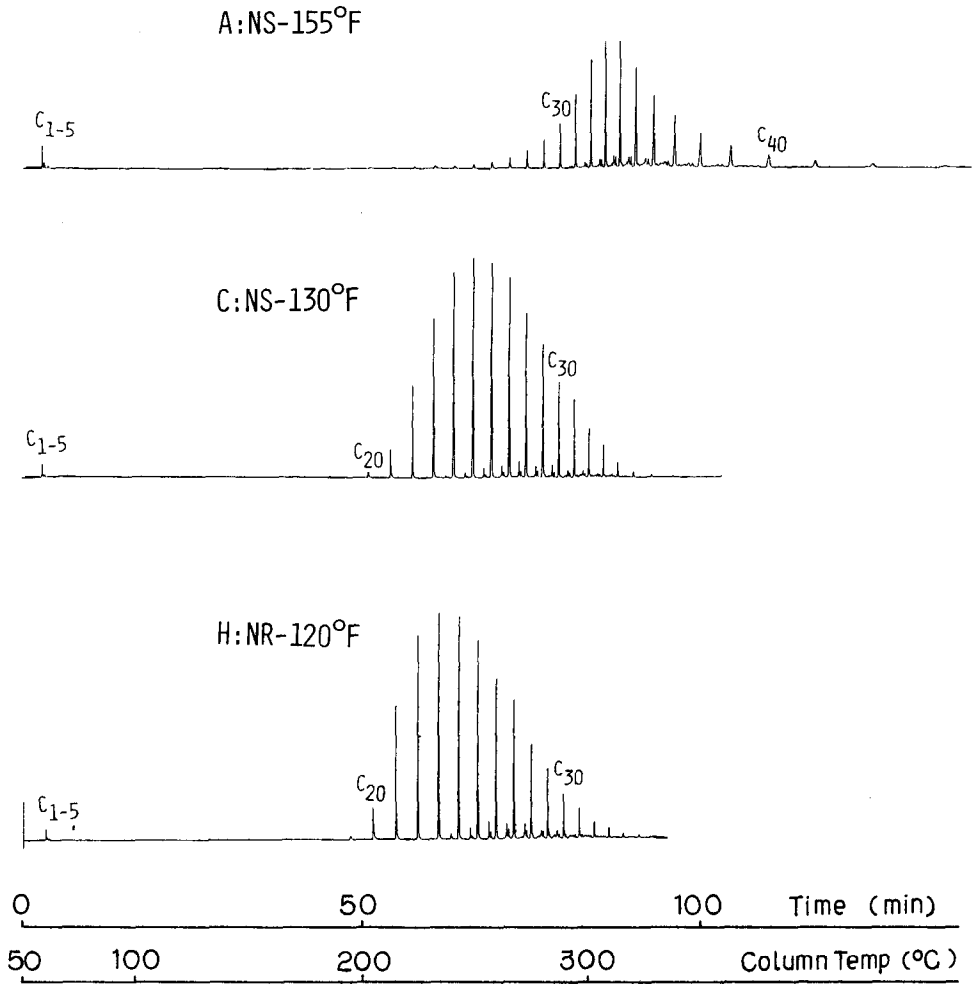

Fig. 7. Chromatograms of paraffin waxes.

dicating that this wax was synthesized by polymerization of ethylene monomers. Small peaks of odd-C *n*-alkanes are also observed, although isoalkanes are rarely seen. Using eqn. 1, the number-average molecular weight of this wax was calculated to be 507, which is very close to the reported value (500). Polywax 655 and Polywax 1000 are basically the same types of waxes as Polywax 500. Like the chromatogram of Polywax 500, large peaks of even-C *n*-alkanes are observed on these chromatograms, although C_1–C_5 thermal decomposition products and the odd-C *n*-alkanes are fairly abundant. These data suggest that thermal decomposition is significant in these instances owing to their higher average molecular weight. Therefore, accurate calculations of $\bar{M}_n$ could not be made for these higher-molecular-weight waxes. Fig. 10 shows the relationships between the observed $\bar{M}_n$ and the relative peak areas of the C_1–C_5 components for the paraffin waxes and Polywax 500. The fact that the relative peak areas of the C_1–C_5 components increase almost linearly with increasing $\bar{M}_n$ suggests

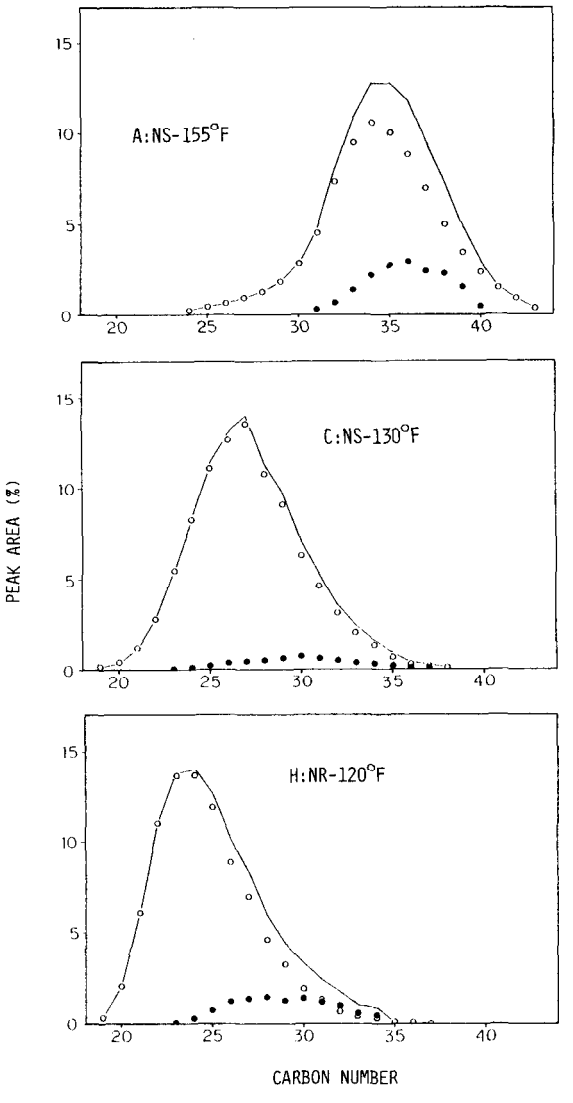

Fig. 8. Component distributions of paraffin waxes. ○, *n*-Alkanes; ●, isoalkanes; ——, total.

that the contribution of thermal decomposition becomes more significant at higher $\bar{M}_n$ of the waxes.

Graphs of melting point, refractive index and specific gravity against $\bar{M}_n$ for the paraffin waxes and Polywax 500 are shown in Figs. 11, 12 and 13, respectively. In every instance there is a fairly good correlation between the physical properties and $\bar{M}_n$, except for Polywax 500 (I). For example, the melting point corresponds well with $\bar{M}_n$, whereas the melting point of Polywax 500 is far above that expected from the data for the paraffin waxes. This phenomenon might be explained by the facts that isoalkanes have lower melting points than the corresponding *n*-alkanes and that

TABLE II

NUMBER-AVERAGE MOLECULAR WEIGHTS AND ISOALKANE CONTENTS OF PARAFFIN WAXES

Wax	*Number-average molecular weight*	*Isoalkane content (%)*
(A) NS-155°F	484	17.5
(B) NS-140°F	409	7.4
(C) NS-130°F	379	5.8
(D) NR-155°F	484	17.3
(E) NR-150°F	451	14.9
(F) NR-140°F	406	7.6
(G) NR-130°F	372	8.1
(H) NR-120°F	350	11.8

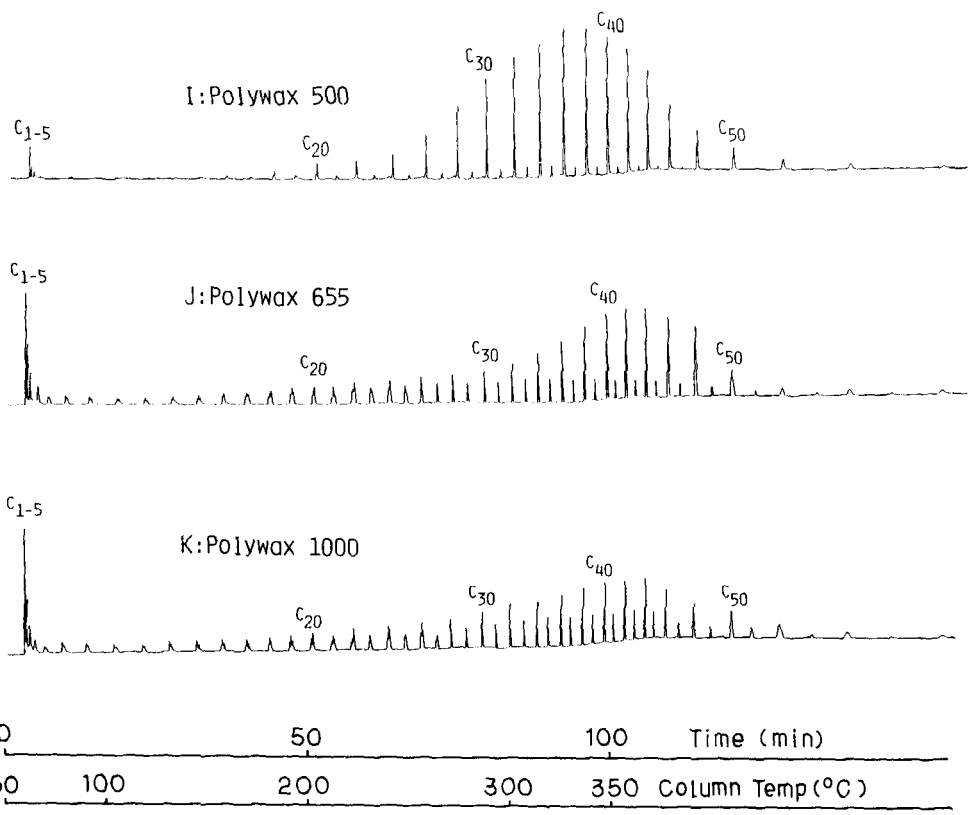

Fig. 9. Chromatograms of synthetic waxes.

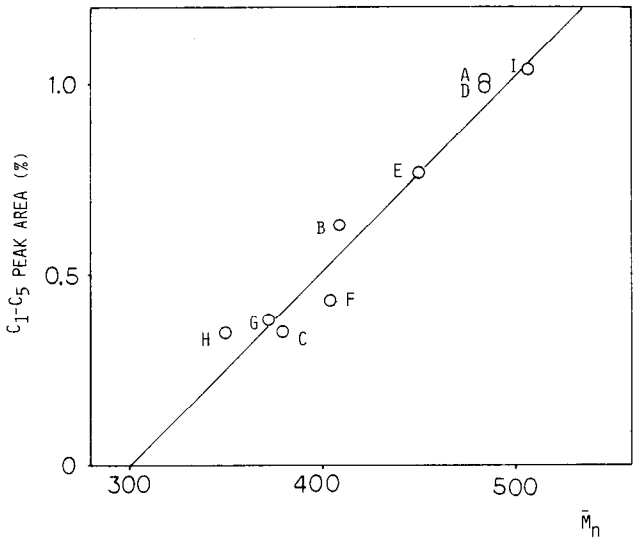

Fig. 10. Relationship between C_1–C_5 peak area and number-average molecular weight.

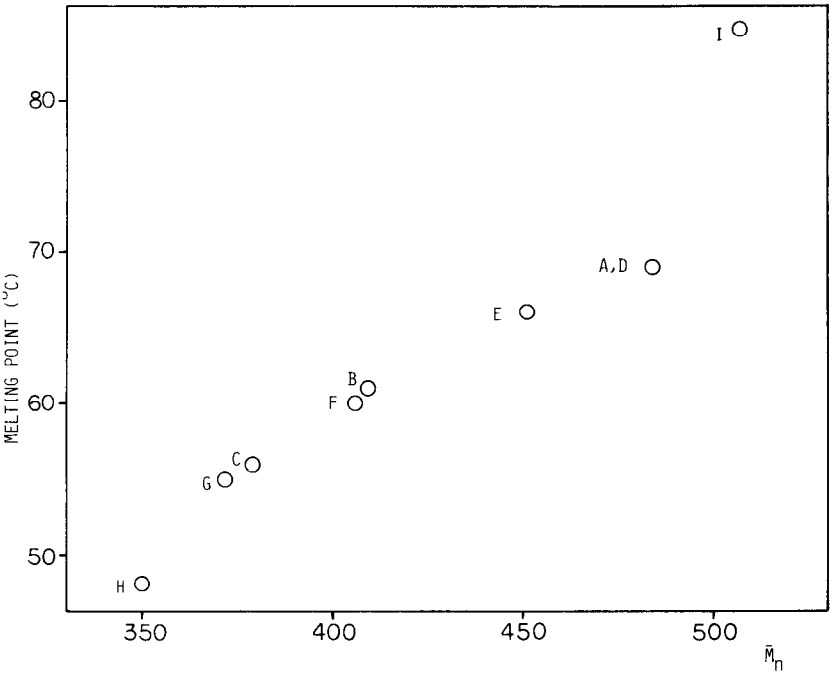

Fig. 11. Relationship between melting point and number-average molecular weight.

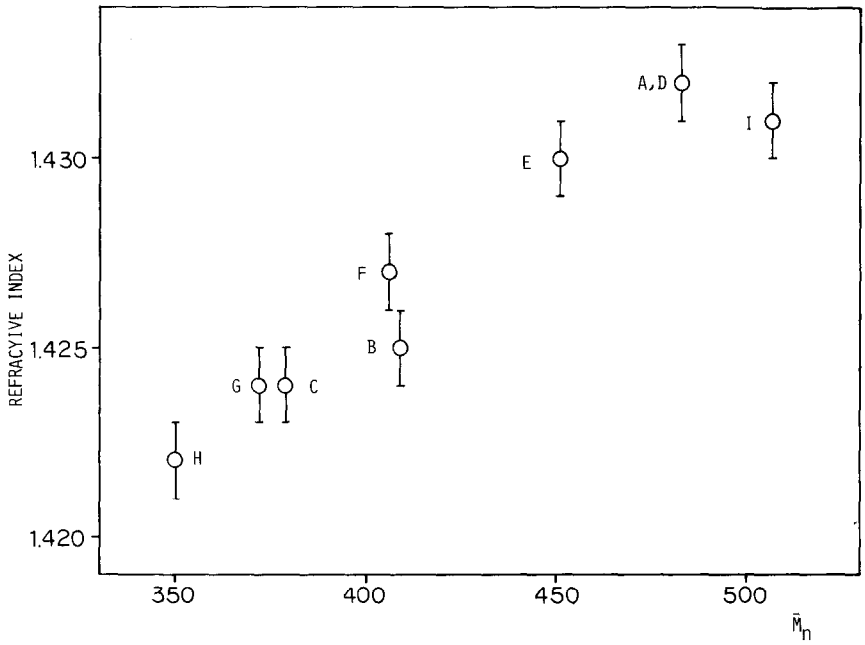

Fig. 12. Relationship between refractive index and number-average molecular weight.

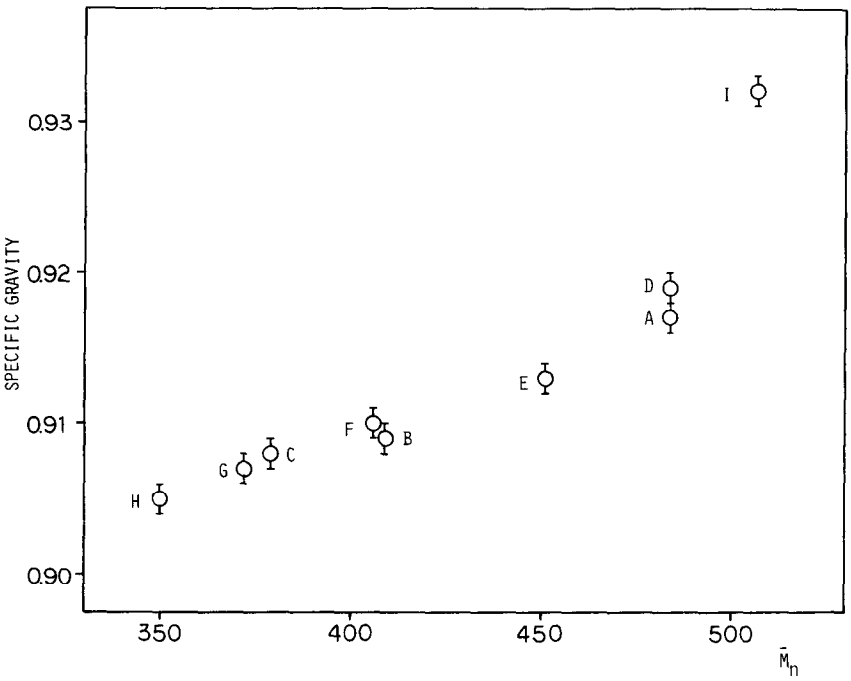

Fig. 13. Relationship between specific gravity and number-average molecular weight.

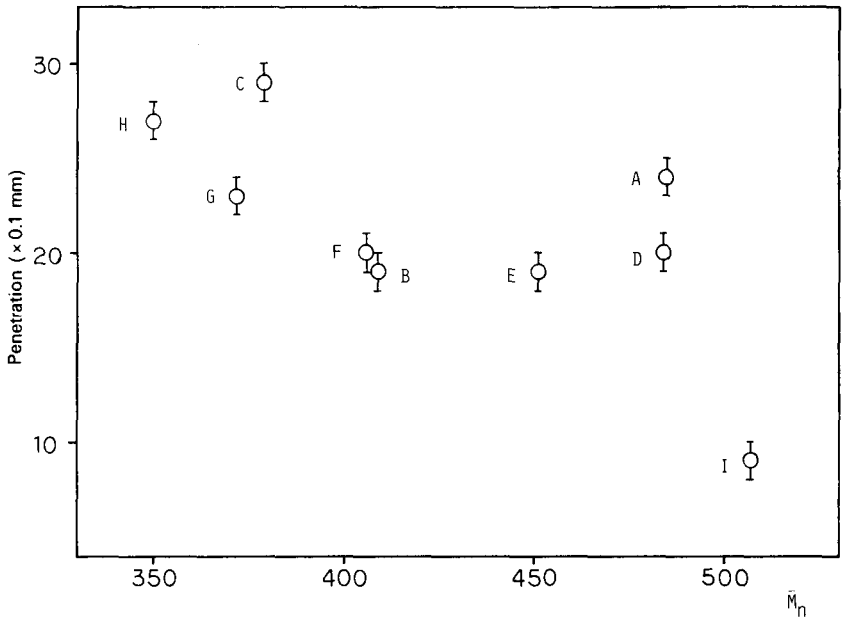

Fig. 14. Relationship between penetration and number-average molecular weight.

Polywax 500 consists of *n*-alkanes whereas the paraffin waxes contain small amounts of isoalkanes.

Fig. 14 shows the penetration data plotted against $\bar{M}_n$. Penetration is a measure of hardness, which may be affected by both the average molecular weight and the content of isoalkanes. Although the penetration values tend to decrease with increase in $\bar{M}_n$, the correlation is not good because of the complex contribution of the isoalkane contents.

Chromatograms of AC-polyethylenes (AC-PE6 and AC-PE615) are shown in Fig. 15, together with that of polyethylene. The patterns of these chromatograms are nearly the same. The large peaks of the C_1–C_5 components and the serial triplets of lower hydrocarbons indicate the significant contribution of thermal decomposition.

Chromatograms of the microcrystalline waxes are shown in Fig. 16. Although the major components of these waxes are said to be branched-chain alkanes, the observed predominant peaks on these chromatograms are *n*-alkanes. Number-average molecular weights of these waxes were estimated to be between 655 and 1000 from the thermal methods discussed later. The total peak areas per unit sample size must be the same for all the waxes, provided that all the components are eluted from the column. However, these values for the microcrystalline waxes were relatively small compared with those for the Polywaxes of similar average molecular weight. Also, the peaks of the pyrolysates on each of these chromatograms are relatively small compared with those for Polywax 655 and 1000. By increasing the vaporizer temperature to 650°C, the total peak area on these chromatograms increased. These results suggest that most of the branched-chain alkanes might not be eluted from the column under given experimental conditions.

Fig. 17 shows the comparative data between the refractive indices and the

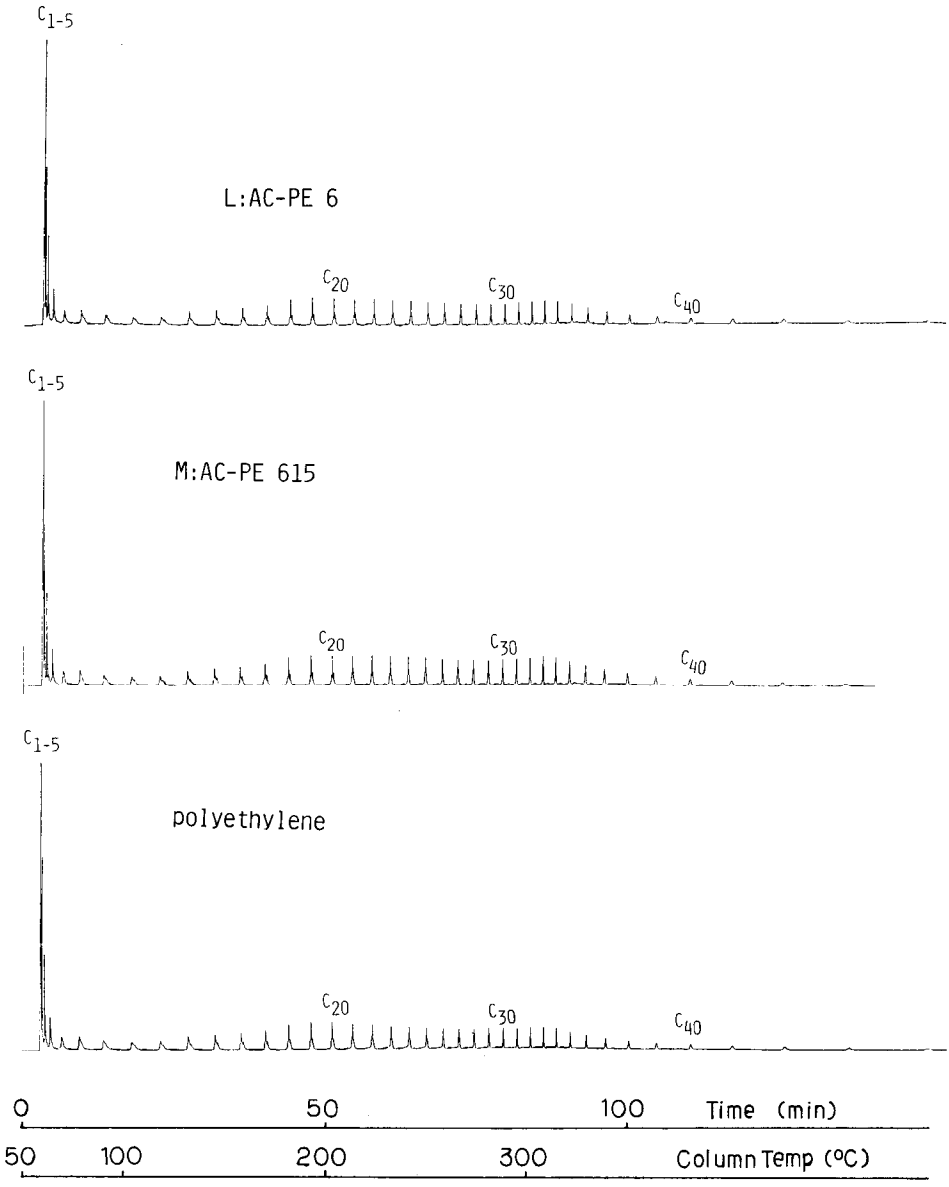

Fig. 15. Chromatograms of polyethylene waxes.

melting points of all the waxes in Table I. Generally, the refractive index increases with increase in melting point. These phenomena could be attributed to their chemical nature, in that they consist almost entirely of high-boiling *n*-alkanes. However, the Polywaxes (I, J, K) have relatively low and constant refractive indices although they have high melting points. In contrast, the relatively high refractive index of the multiwax X-145 (N) might be due to its higher contents of branched-chain alkanes and oils.

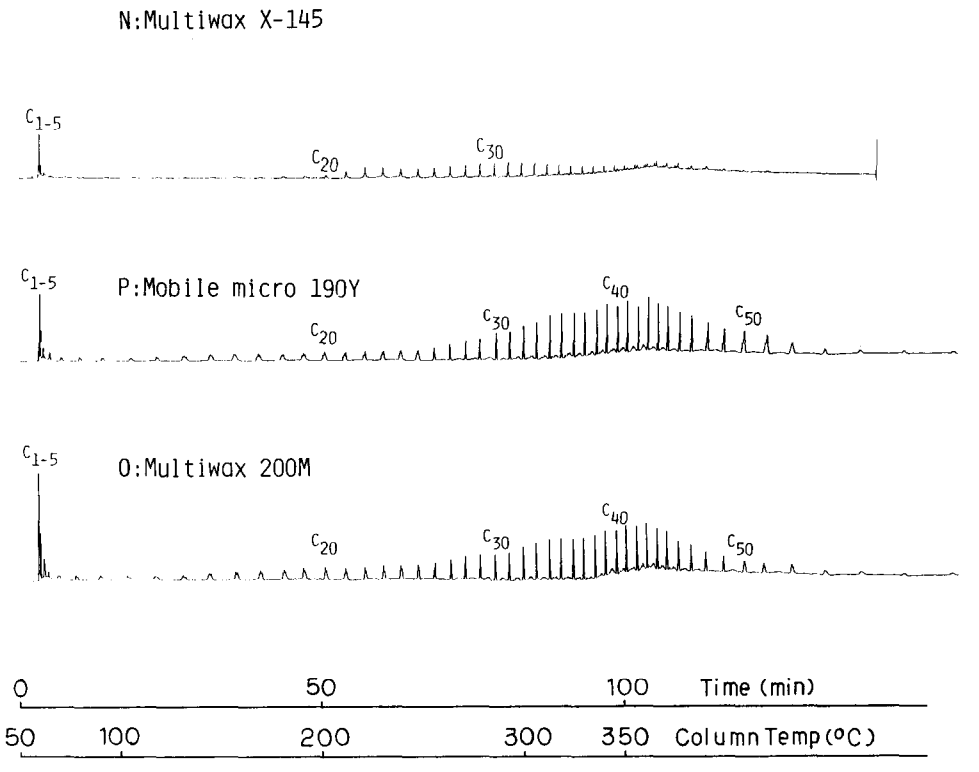

Fig. 16. Chromatograms of microcrystalline waxes.

TGA

TGA curves of some of the waxes in Table I are shown in Fig. 18. These TGA curves should be characteristic of the molecular weight distributions of the waxes. As the average molecular weights of the paraffin waxes (A, B, C and H) increase, the weight loss curves shift to the higher temperature region, while the slopes of these curves remain almost the same. This suggests that the paraffin waxes have nearly the same width of the molecular weight distribution, regardless of their average molecular weights. On the other hand, the weight loss of Polywax 500 (I) starts at a relatively low temperature of 200°C, but it continues up to 450°C with a gentle slope. This indicates that this wax has a fairly wide range of molecular weight distribution. These results are in good agreement with the GC data in Figs. 7 and 9.

The TGA curves of the higher molecular weight waxes generally show weight loss at higher temperatures with gentle slopes, mainly owing to the contribution of thermal decomposition. Number-average molecular weights of the microcrystalline waxes (N, O and P) were estimated to be between 655 and 1000, as their TGA curves show a weight loss between those of Polywax 655 (J) and Polywax 1000 (K).

Measurement of thermal vaporization curves with an FID

Fig. 19 shows the thermal vaporization curves of typical waxes at 400°C, obtained with the device shown in Fig. 3. In this method, the vaporized sample com-

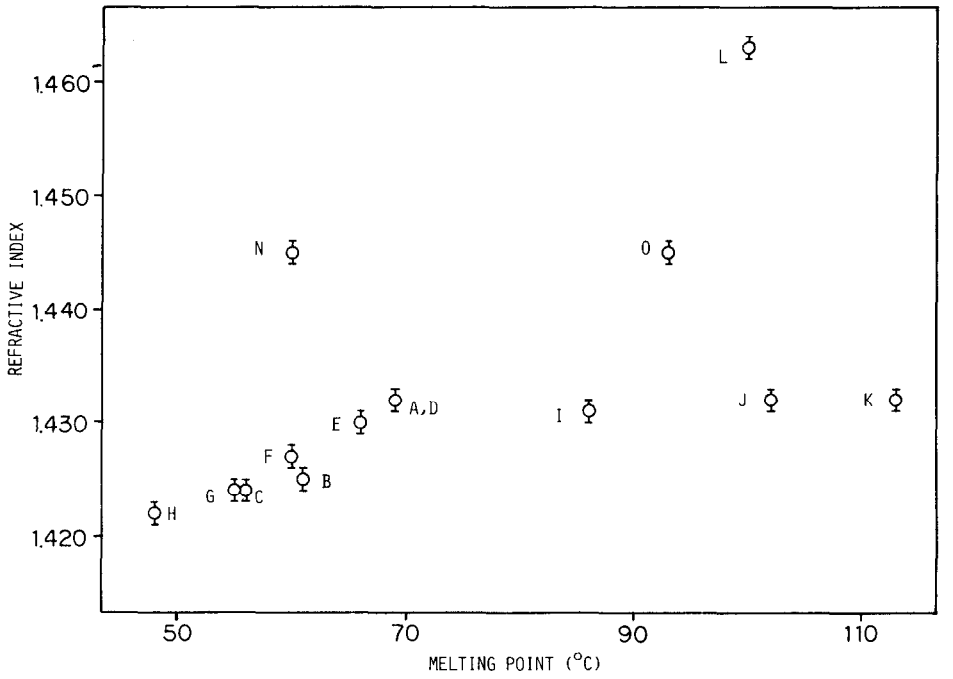

Fig. 17. Relationship between refractive index and melting point.

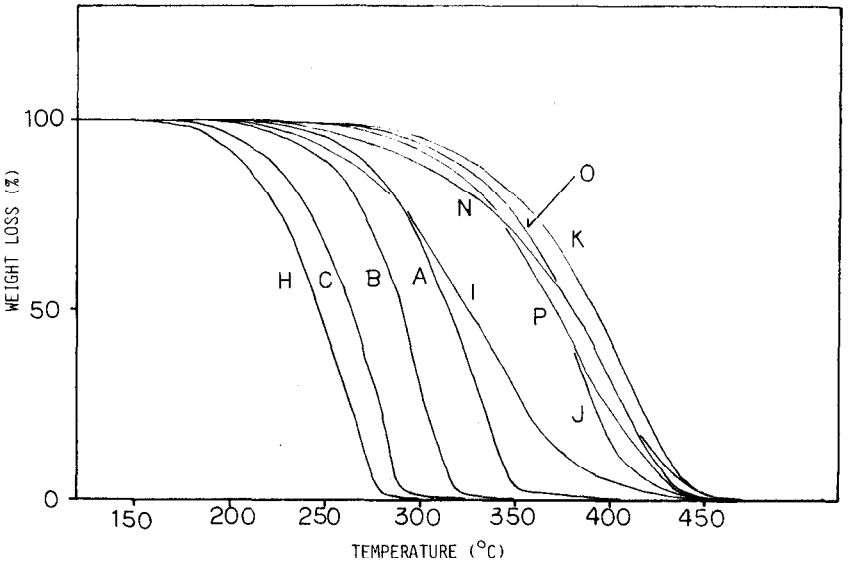

Fig. 18. TGA curves of waxes.

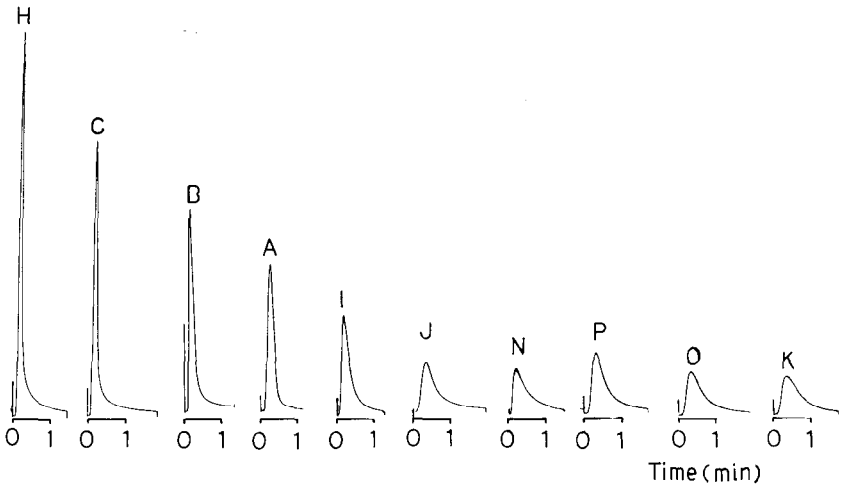

Fig. 19. Vaporization curves of waxes, detected by FID.

ponents were detected directly with the FID without any chromatographic separation. The resulting thermograms might correspond to the differential curves of the TGA thermograms obtained at a constant temperature (400°C). Therefore, the profiles of these thermograms reflect the average molecular weight and the molecular weight distributions of the wax samples.

As an example, the number-average molecular weight of the microcrystalline waxes (N, P and O) were estimated to be between 655 and 1000, as the profiles of the thermograms are between those of Polywax 655 (J) and Polywax 1000 (K).

REFERENCES

1 H. Bennette, *Industrial Waxes*, Vol. 1, Chemical Publishing Co., New York, 1975.
2 D. J. Harmon, *J. Liq. Chromatogr.*, 1 (1978) 231.
3 F. J. Ludwig, *Anal. Chem.*, 37 (1965) 1737.
4 R. Miller and G. Dawson, *Thermochim. Acta*, 41 (1980) 93.
5 M. J. O'Neal, Jr., and T. P. Wier, Jr., *Anal. Chem.*, 23 (1951) 830.
6 F. J. Ludwig, *Anal. Chem.*, 37 (1965) 1732.
7 J. F. Lawrence, J. R. Iyengar, B. D. Page and H. B. S. Conacher, *J. Chromatogr.*, 236 (1982) 403.
8 Y. Sugimura and S. Tsuge, *Anal. Chem.*, 50 (1978) 1968.
9 M. Seeger and R. J. Gritter, *J. Polym. Sci.*, 15 (1977) 1393.